A downscaling method for distributing surface soil moisture within a microwave pixel: application to the Monsoon '90 data

O. Merlin

Centre d'Etudes Spatiales de la Biosphère, Toulouse, France

A. Chehbouni

Centre d'Etudes Spatiales de la Biosphère, Toulouse, France

Y.H. Kerr

Centre d'Etudes Spatiales de la Biosphère, Toulouse, France

D.C. Goodrich

USDA-ARS Southwest Watershed Research Center, Tucson AZ, USA

Abstract

A downscaling method of the microwave surface soil moisture is applied to the PBMR data collected during the Monsoon '90 experiment. The downscaling method requires (1) the coarse resolution microwave observation (2) the distribution at fine scale of soil temperature and (3) the distribution at fine scale of the surface conditions composed of atmospheric forcing and the parameters involved in the modeling of land surface-atmosphere interaction. During the Monsoon '90 experiment,

eight ground-based meteorological and flux stations were operating over the 150 km^2 study area simultaneously with the acquisition of the aircraft-based L-band PBMR data. The heterogeneous scene is hence composed of eight sub-pixels and the microwave pixel is generated by aggregating the microwave emission of all sites. The results show a good agreement between the downscaled and ground-based soil moisture as long as the intensity of solar radiation is sufficiently high to use the soil temperature as a tracer of the spatial variability of surface soil moisture.

Key words: downscaling, surface soil moisture, passive microwave remote sensing, SMOS mission, hydrology, Monsoon '90 experiment

---

1 Introduction

Passive microwave remote sensing has demonstrated the capability to capture the high temporal variability of the near-surface soil moisture over continental surfaces. However, the use of these data in the field of hydrology is limited by the poor spatial resolution obtained with the current and near-future generation of spaceborne radiometers. As mentioned in Engman (1991) and more recently in Entekhabi et al. (1999), the use of space-based passive microwave data in hydrological modeling is not straightforward because of the scale discrepancy between the typical microwave resolution (several tens of km) and the scale at which most hydrological processes occur (about one km).

In this context, the application of passive microwave radiometry in agriculture and water resources requires the disaggregation (improve the resolution) of the passive microwave soil moisture. This has been a major motivation for developing different downscaling methods to distribute fine scale soil moisture within a microwave pixel. Recent works on this subject use fractal interpo-

lation methods with fine scale surface information (Kim and Barros (2002)), an interpolation method of passive microwave data with fine scale active microwave data (Bindlish and Barros (2002)), a distributed hydrological model with local information on topography (Pellenq et al. (2003)) or linear regressions between a vegetation index, surface temperature and surface soil moisture with fine scale optical data (Chauhan et al. (2003)).

In the scope of the Soil Moisture and Ocean Salinity (SMOS) mission (Kerr et al. (2001)), a new downscaling method based on fine scale optical data was developed by Merlin et al. (2005) to improve the spatial resolution of the SMOS surface soil moisture. The SMOS mission, scheduled for launch in early 2007, is based on a dual polarized L-band radiometer with significant capabilities in terms of multi-angular viewing configurations. This allows for simultaneously retrieving surface soil moisture and vegetation water content with a spatial resolution of approximately 40 km (Wigneron et al. (2000)).

To downscale the 40 km resolution SMOS soil moisture, the method of Merlin et al. (2005) operates in two successive steps. In the first step, a spatial distribution of surface soil moisture is estimated from the radiometric soil temperature derived from fine scale (typically 1 km resolution) optical data. The distribution is then a function of two parameters: the microwave scale soil moisture W_{SMOS} and a first-order parameter f_1 fixing the range covered by downscaled values. In the second step, the distribution obtained in step 1 is calibrated at microwave scale by inverting both parameters W_{SMOS} and f_1 from multi-angular SMOS observation.

Based on the Southern Great Plains '97 data (Jackson et al. (1999)), Merlin et al. (2005) showed that the radiometric soil temperature derived from

thermal/optical data can be used to describe the spatial variability of L-band microwave soil moisture. The objective of this paper is to validate with the Monsoon '90 data (Kustas et al. (1991); Kustas and Goodrich (1994)) two key steps of the disaggregation algorithm which were not tested with real data by Merlin et al. (2005), in particular the use of a land surface model within the disaggregation and the ability of the algorithm to invert the pair (W_{SMOS}, f_1) from multi-angular microwave data.

During the Monsoon '90 experiment, eight ground-based meteorological and flux (METFLUX) stations were operating over the 150 km^2 study area simultaneously with the acquisition of the aircraft-based L-band PBMR data. In this study, a heterogeneous coarse resolution microwave pixel is generated by aggregating the eight PBMR pixels located at the eith METFLUX sites. The performance of the method is then assessed by comparing the downscaled surface soil moisture to ground-based measurements at each METFLUX site and for each day of PBMR observation.

In the disaggregation method, the spatial variability of surface soil moisture within a microwave pixel is explained with fine scale optical data. As the triangular method of Chauhan et al. (2003) is based on the same local information, a comparison between both approaches is proposed in section 2. In section 3, the data collected during the Monsoon '90 experiment are described and the setup of a coarse resolution microwave pixel used as input of the dowscaling method is detailed. The models are then presented in section 4 before the main steps of the method of Merlin et al. (2005) are reminded. Finally in section 5, the downscaling scheme is applied to the generated microwave pixel and the downscaled surface soil moisture is compared to ground-based measurements.

2 Comparison with the triangular method

The downscaling method adopted in this paper is fully described in Merlin et al. (2005) (M05). As there are a few similarities with the triangular method presented in Chauhan et al. (2003) (C03), a comparison of both approaches is provided below.

Both C03 and M05 use fine scale remotely sensed data in the visible, near-infrared and thermal infrared to describe the spatial variability of the microwave soil moisture at fine scale. Basically, the radiometric surface temperature T_{rad} is derived from thermal infrared data and correlated in space with the microwave soil moisture W. Visible/near-infrared data are then used to account for the effect of the vegetation heterogeneity in the spatial correlation between T_{rad} and W.

In both methods, the spatial correlation between the radiometric surface temperature T_{rad} and the microwave soil moisture W is explained by the capacity of the surface to counter the increase of its physical temperature by evaporating the soil water content (surface thermal inertia). To account for the dependence of the surface thermal inertia to surface variables other than W, auxiliary information at optical resolution are used. In particular, C03 uses NDVI to calibrate empirically the correlation between T_{rad} and W for different vegetation covers and M05 uses the fractional vegetation cover to invert the radiometric soil temperature, which is assumed to be more directly linked to W than the radiometric surface T_{rad}.

Beyond these similarities, M05 differs from C03 in three main points. First, M05 is based on physical models whereas the disaggregation strategy of C03

is empirically-based. Second, it uses all the data available at optical resolution (soil texture, atmospheric forcing and all the soil and vegetation characteristics involved in the modeling of land surface-atmosphere interaction) and not uniquely a vegetation index as in C03. Third, M05 requires a microwave observation composed of at least two independent (angular) brightness temperatures (i.e. a SMOS type pixel). In C03, a unique brightness temperature is sufficient.

3 The data

The data collected during the Monsoon '90 campaign are used. In this section, the Monsoon '90 data are described and the setup of the microwave pixel used as input of the downscaling method is detailed.

3.1 The Monsoon '90 data

The Monsoon '90 Experiment was conducted during the summer 1990 over an arid watershed in south central Arizona in the USA (Kustas and Goodrich (1994)). The purpose of the experiment was to observe the moisture fluxes in an arid climate during a drydown and the role of remote sensing in determining these fluxes. A network of eight meteorological surface energy flux (METFLUX) stations covering the main study area (about 150 km^2) were situated in grass-dominated and shrub-dominated ecosystems and in the transition zones containing both vegetation types. Each METFLUX site measured continuously: the ground 0–5 cm soil moisture, the ground soil temperature at different depths, meteorological conditions at screen height composed of air

temperature, relative humidity, wind speed and solar radiation. Soil texture was characterized by ground-based measurements of sand and clay percentages, and canopy height was estimated with Weltz et al. (1994).

As part of the Monsoon '90 campaign, the NASA PushBroom Microwave Radiometer (PBMR) was flown on six flights of the C-130 aircraft during a 10-days period in July and August of 1990. The date, time and cloud cover conditions of each of the six PBMR flights are presented in Table 1. The objective was to map the surface brightness temperature at a wavelength of 21-cm (L band) and to infer surface soil moisture from these data. The 4 beams of PBMR instrument point at ± 8 and ± 24 degrees incidence angle with a 3 dB beam width of about 0.3 altitude. For Monsoon '90 the PBMR flights were at an altitude of 600 m, which yielded an IFOV of 180 m. Available PBMR data of the Monsoon '90 experiment are provided under the form of nadir brightness temperatures. To create the images of the brightness temperature at nadir, the outer beams were corrected for incidence angle effects by multiplying them by the ratio of the average of the center beam to the outer beam on each side.

3.2 Generate a time-series of heterogeneous microwave pixels

The data collected during the Monsoon '90 experiment are particularly suitable for testing the downscaling method M05. All the required input data are available at the time of L-band PBMR observations. In addition, the spatial variations of rainfall during the 10-days period of PBMR observations (from Julian day 212 to Julian day 221) caused a significant variability of soil moisture within the study area. The conditions particularly dry on Julian day (JD) 212, and particularly wet on JD 214 and 216, and the drydown process

from JD 217 to the end of PBMR missions (on JD 221) allow to apply the downscaling method under different surface and atmospheric conditions.

A time-series of heterogeneous microwave pixels is generated from PBMR data. For each day of PBMR observation, a microwave pixel is generated by aggregating the eight PBMR pixels located at the eight METFLUX sites. The heterogeneity within the microwave pixel is hence characterized locally by each METFLUX station providing ground-based measurements of the 0–5 cm soil moisture, the soil temperature at different depths and atmospheric conditions. One should note that the input of radiometric soil temperature is not used in this application, and is replaced by the ground-based soil temperature measured locally by the eight METFLUX stations.

In the next sections, the scale of the PBMR pixels composing the microwave pixel (associated with the eight METFLUX sites) will be referred to "local scale".

4 Method

The two models used in the analysis are described and the main steps of the downscaling method are presented.

4.1 Models

Two models are used by the downscaling method: an L-band radiative transfer model and a land surface model. A description of both models is given below.

4.1.1 A radiative transfer (RT) model

A radiative transfer model is used by the downscaling method to simulate the L-band brightness temperatures remotely sensed by PBMR instrument during the Monsoon '90 experiment.

Over the 10-days period of PBMR observations, Schmugge et al. (1994) showed that there does not appear to be any correlation of the variation of the slopes of the relation PBMR brightness temperature/ground-based soil moisture with any soil or vegetation parameters such as sand, clay, percentage rock or biomass. As a matter of fact, the physically-based tau-omega formalism (Mo et al. (1982); Brunfeldt and Ulaby (1984); Ulaby et al. (1986)) could not be used to model the L-band surface emission. However, the results of Schmugge et al. (1994) on a site-by-site basis showed excellent correlation of PBMR brightness temperatures with ground-based soil moisture. In this study, the results of Schmugge et al. (1994) are therefore used to build an empirical relationship between PBMR brightness temperatures and ground-based measurements of soil moisture on each METFLUX site.

The formulation of the angular brightness temperature TB^{α} at the incidence angle α is given by:

$$TB^{\alpha} = a^{\alpha}W + b^{\alpha} \tag{1}$$

with W the 0–5 cm soil water content and a^{α} and b^{α} two angular parameters. The radiative transfer (RT) model simulates the microwave observation TB composed of the nadir brightness temperature $TB^{\perp}$ and an oblique brightness

temperature $TB^{\angle}$:

$$TB = (TB^{\perp}, TB^{\angle}) = \mathbf{RT}(W, X) \tag{2}$$

with $X = (a^{\perp}, b^{\perp}, a^{\angle}, b^{\angle})$ a vector composed of the four angular parameters.

The calibration of RT model on the Monsoon '90 data is done in two steps. The first step consists of using the Monsoon '90 nadir brightness temperature to calibrate parameters $a^{\perp}$ and $b^{\perp}$. Assuming that ground-based measurements of surface soil moisture are spatially consistent with the 180 m resolution PBMR nadir brightness temperature, parameters $a^{\perp}$ and $b^{\perp}$ are evaluated for each METFLUX site by minimizing the error on the simulated nadir brightness temperatures. Only the three first days of PBMR observations are used for the calibration (JDs 212, 214 and 216).

The second step of the calibration of RT model consists of calibrating parameters $a^{\angle}$ and $b^{\angle}$. This requires to generate an oblique brightness temperature $TB^{\angle}$ from the Monsoon '90 nadir brightness temperature. Given that PBMR instrument is composed of four beams pointing at ± 8 and ± 24, one is able to synthetize a 24 incidence angle brightness temperature from the nadir brightness temperature $TB^{\perp}$ (taken at 8 incidence angle) and the angular effects sensed by the instrument. In practice, the oblique brightness temperature $TB^{\angle}$ is computed by dividing the Monsoon '90 nadir brightness temperature by the daily mean directional ratio sensed by PBMR instrument. Parameters $a^{\angle}$ and $b^{\angle}$ are then estimated for each METFLUX site by minimizing the root mean square difference between simulated and generated oblique brightness temperatures with the data subset composed of JDs 212, 214 and 216.

Calibration parameters are presented in Table 2. Figure 1 illustrates the cal-

ibration results in terms of the simulated brightness temperature and the simulated nadir-oblique brightness temperature difference. In (a), the brightness temperature simulated by RT model is plotted versus PBMR data. The calibration error is found to be 4.5 K for the entire dataset. In (b), the daily difference ($TB^{\perp} - TB^{\angle}$) is plotted as function of the daily mean soil moisture for JDs 212, 214, 216, 217, 220 and 221. It can be seen that the angular effect increases with surface soil moisture. This information is specifically used by the method of Merlin et al. (2005) to constrain properly the disaggregated values at the scale of microwave resolution.

4.1.2 A land surface (LS) model

A land surface model is used by the downscaling method to simulate the soil surface temperature under different surface conditions within the microwave pixel.

The land surface model used for the application to the Monsoon '90 data is the so-called N95 surface model developed by Norman et al. (1995), revised by Kustas et al. (1998) and improved with Kustas and Norman (1999). Briefly, a dual-source model treating the energy balance of the soil/substrate and vegetation was developed to use radiometric surface temperature observations at zenith view angle (Norman et al. (1995)) and remotely sensed images of near-surface soil moisture (Kustas et al. (1998)) for estimating the soil energy balance over the watershed of the Monsoon '90 experiment. In this study, the model revised by Kustas et al. (1998) is preferred because the heterogeneity of the 0–5 cm soil moisture in accounted for in the estimation of soil temperature. The model formulation computes explicitly the soil evaporation as a function

of the resistance of the surface soil layer to water vapor transfer. The resistance of surface soil layer r_{ss} is parameterized with surface soil moisture W (Sellers et al. (1992)):

$$r_{ss} = \exp(A - BW/W_{sat}) \tag{3}$$

with A and B two calibration parameters and W_{sat} the saturated volumetric water content, parameterized with sand fraction following Noilhan and Mahfouf (1996). The land surface (LS) model is used to simulate radiometric soil temperature T_s:

$$T_s = \mathbf{LS}(W, Y) \tag{4}$$

given the 0–5 cm soil water content W and the vector $Y = (S, T_a, Rh_a, u_a, sand, A, B, h_c, LAI)$ composed of: incoming solar radiation S, air temperature T_a, relative humidity of air Rh_a, wind speed u_a, sand fraction, parameters A and B, canopy height h_c and LAI.

The calibration of LS model on a site-by-site basis is performed on parameters A and B by minimizing the error on the simulated soil temperature in the period JD 212-216. A mean value estimated to 1 was taken for LAI (Daughtry et al. (1991)). The ensemble of parameters other than h_c, *sand*, A and B were fixed to the homogeneous values estimated in Kustas et al. (1998) and Kustas and Norman (1999) for the study area. The dataset of ground-based soil temperature is generated by averaging the 5 independent ground-based measurements of soil temperature (3 at -2.5 cm and 2 at -5 cm) acquired at each METLFLUX site between 10 a.m. and 2 p.m. (12 acquisitions per day and per site) during the 10-days period of PBMR observation. The values of

parameters A and B are presented in Table 2 for the eight METFLUX sites. The soil surface temperature simulated by LS model is plotted versus ground-based measurements in Figure 2. The root mean square error on the simulated soil temperature in the whole period (JD212-221) is found to be 3.5 K.

4.2 Downscaling Method

The method M05 downscales the microwave surface soil moisture in two successive steps. In the first step, the local information provided by the eight METFLUX stations (ground-based soil temperature, atmospheric conditions, soil and vegetation characteristics) are used to describe the spatial variability of surface soil moisture within the microwave pixel. A soil moisture distribution is then expressed as function of two parameters: the microwave scale soil moisture W_{SMOS} and a first-order parameter f_1 called the contrast parameter of the distribution. In the second step, the distribution obtained in step 1 is calibrated at the scale of the microwave pixel by inverting both parameters W_{SMOS} and f_1 from bi-angular microwave observation.

The two main steps of the downscaling method (i.e. estimate a distribution, and calibrate the distribution) are described below and shown in the diagram of Figure 3.

4.2.1 Estimate a soil moisture distribution

The first step of the downscaling method consists of estimating a distribution of surface soil moisture from the ground-based soil temperature measured locally at the METFLUX sites. One difficulty to link the ground-based soil

temperature T_s to the microwave soil moisture W is the fact that the spatial correlation between T_s and W depends on other surface variables such as soil texture, atmospheric forcing and soil/vegetation characteristics (i.e. all the variables contained in Y). To overcome this difficulty, the downscaling method uses LS model and the knowledge of the local surface conditions Y within the microwave pixel to extract specifically the information on W contained in T_s. One is then able to link the spatial variability of surface soil moisture to the known variability of ground-based soil temperature. Both points are successively described below.

4.2.1.1 Extract the information contained in T_s: to extract the information on W contained in T_s, the downscaling method simulates the variability of ground-based soil temperature that is specifically due to the variables contained in Y. In practice, two soil temperatures are simulated with LS model. First, LS model is used to simulate the soil surface temperature noted T_s associated with the local ground-based surface conditions Y^m (exponent ^{m} refers to measured variables):

$$T_s = \mathbf{LS}(W, Y^m) \tag{5}$$

Second, LS model is used to simulate the soil surface temperature noted $\overline{T_s}$ associated with the surface conditions aggregated at the scale of the microwave pixel $< Y >$:

$$\overline{T_s} = \mathbf{LS}(W, < Y >) \tag{6}$$

where $< Y >$ is the average of the local surface conditions Y^m. The difference $(T_s - \overline{T_s})$ represents the predicted contribution of soil temperature that is due

to the varibility of Y within the microwave pixel. By substracting $(T_s - \overline{T_s})$ to the ground-based soil temperature T_s^m, a theoretical variable noted $\overline{T_s^m}$ is obtained:

$$\overline{T_s^m} = T_s^m - (T_s - \overline{T_s}) \tag{7}$$

As the function written in (8) is a projection, the variable $\overline{T_s^m}$ is called Projected soil temperature. By definition, the spatial variability of Projected soil temperature is attributed uniquely to the spatial variability of surface soil moisture. The downscaling method can therefore use $\overline{T_s^m}$ to explain the spatial variability of W.

4.2.1.2 Estimate a spatial distribution: a spatial distribution of surface soil moisture is finally expressed by linking the downscaled soil moisture W to Projected soil temperature $\overline{T_s^m}$ at first order:

$$W = f_0 + f_1 \overline{T_s^m} \tag{8}$$

with f_0 and f_1 two parameters defined at the scale of the microwave pixel.

4.2.2 Calibrate the distribution

The second step of the downscaling method aims to calibrate the soil moisture distribution of (8) at the scale of the microwave pixel. In practice, the calibration of parameters f_0 and f_1 is performed by looking for a particular solution of the pair (f_0, f_1) such that the microwave scale soil moisture W_{SMOS} appears in the expression of the downscaled soil moisture W. Both parameters W_{SMOS} and f_1 are then inverted by matching the microwave observation simulated

from the downscaled soil moisture and the measured microwave observation.

4.2.2.1 Find a particular solution: a particular solution of the pair (f_0, f_1) is set to make the microwave scale soil moisture W_{SMOS} appear in the expression of the downscaled soil moisture. Let f_0 such as:

$$f_0 = W_{SMOS} - f_1 < \overline{T_s^m} > \tag{9}$$

where $< \overline{T_s^m} >$ is the Projected soil temperature aggregated (linearly) over the microwave pixel.

4.2.2.2 Express the downscaled soil moisture: by replacing f_0 in (8) by the expression of (9), a new expression of the downscaled soil moisture is obtained as a function of the pair (W_{SMOS}, f_1):

$$W(W_{SMOS}, f_1) = W_{SMOS} + f_1(\overline{T_s^m} - < \overline{T_s^m} >) \tag{10}$$

In this expression, W_{SMOS} determines the effective level of the distribution at microwave resolution whereas the contrast parameter f_1 fixes the range covered by downscaled values.

4.2.2.3 Build a cost function: a cost function is built in order to evaluate the distance between the microwave observation simulated from the downscaled soil moisture of (10) and the measured microwave observation. The cost function F is defined as:

$$F(W_{SMOS}, f_1) = \left\| < \mathbf{RT}(W, X^m) > - TB^m_{SMOS} \right\|^2 \tag{11}$$

with W the fine scale soil moisture expressed in (10), TB^m_{SMOS} the measured microwave observation and $< \mathbf{RT}(W, X^m) >$ the average of simulated local observations. The cost function F is then minimized to invert the pair (W_{SMOS}, f_1). Note that the problem of retrieving the pair (W_{SMOS}, f_1) from bi-angular microwave data is theoretically well defined because the number of independent microwave observations contained in TB^m_{SMOS} is equal to the number of unknows, which is two.

4.2.2.4 Invert W_{SMOS}: the microwave scale soil moisture W_{SMOS} is inverted by setting $f_1 = 0$:

$$W^{inv}_{SMOS} = \mathrm{Min}_{W_{SMOS}} F(W_{SMOS}, 0) \tag{12}$$

with W^{inv}_{SMOS} the inverted SMOS scale soil moisture, which minimizes the cost function F.

4.2.2.5 Invert f_1: the contrast parameter f_1 is inverted by fixing $W_{SMOS} = W^{inv}_{SMOS}$:

$$f^{inv}_1 = \mathrm{Min}_{f_1} F(W^{inv}_{SMOS}, f_1) \tag{13}$$

with f^{inv}_1 the inverted value of contrast parameter, which minimizes the cost function F. At this point, the soil moisture distribution is entirely determined and is characterized by the pair $(W^{inv}_{SMOS}, f^{inv}_1)$. Note that the description given above is an outline of the method and readers are encouraged to refer to Merlin et al. (2005) for an understanding in depth of the different steps of the algorithm.

5 Application

The downscaling method is applied to the time-series of microwave pixels generated from the Monsoon '90 data. To account for uncertainity in input data, an ensemble of input data is first generated for the six days of PBMR observation. Then, the usefullness of the projection technique of gound-based soil temperature is checked by comparing the correlation ground-based soil temperature/soil moisture and the correlation Projected soil temperature/soil moisture for the entire input dataset. Finally, the results of the disaggregation are presented and statistically compared to the ground-based measurements of surface soil moisture at each METFLUX site and for each PBMR mission.

5.1 Generate an ensemble of input data

A SMOS type microwave observation is generated on JDs 212, 214, 216, 217, 220 and 221 by aggregating the Monsoon'90 brightness temperature acquired at the eight METFLUX sites. The microwave observation TB^m_{SMOS} is composed of two angular (nadir and oblique) brightness temperatures. The nadir brightness temperature ${TB^m_{SMOS}}^{\perp}$ is generated by averaging the Monsoon '90 nadir brightness temperatures over the METFLUX sites. The oblique brightness temperature is generated by dividing the Monsoon '90 nadir data by the daily angular effect sensed by PBMR instrument. Because the angular brightness data extrapolated from the nadir looking PBMR observations do not provide independent data set of brightness temperatures in terms of measurement noise, a Gaussian noise of 2 K is added on the oblique brightness temperature. The microwave scale oblique brightness temperature ${TB^m_{SMOS}}^{\angle}$

is then generated by averaging the oblique data at all sites. A set of 20 independent oblique observations is generated for each PBMR mission.

To account for uncertainity in ground-based input data, the data collected between 10 a.m. and 2 p.m. from JD 212 to JD 221 are used. Within the four hours-period, 12 acquisitions of ground-based soil temperature T_s^m and surface conditions Y^m were sampled with a time step of integration of 20 minutes. The 12 measurements are therefore independent with respect to measurement noise.

The ensemble of input data is therefore composed of $20 \times 12 = 240$ independent datasets for each of the six PBMR missions. This allows for the provision of statistical results in terms of mean and standard deviation of the 240 downscaled values of surface soil moisture.

5.2 Projection of soil temperature

An illustration is given of the projection technique. It is reminded that the downscaling method projects ground-based soil temperature with equation (7) to use ground-based soil temperature as a tracer of the spatial variability of surface soil moisture within the microwave pixel. In fact, the projection aims to improve the correlation between soil temperature and soil moisture. To check the usefullness of the projection of ground-based soil temperature, Projected soil temperature is computed with the entire input dataset and the correlation between Projected soil temperature and surface soil moisture is compared to the correlation between ground-based soil temperature and surface soil moisture. Note that the aggregated surface conditions $< Y >$

involved in (6) are computed by averaging the local surface conditions Y^m of the entire dataset.

In Figure 4 are plotted in (a) ground-based soil temperature versus surface soil moisture and in (b) Projected soil temperature $\overline{T_s^m}^{(1)}$ versus surface soil moisture. Note that Projected soil temperature $\overline{T_s^m}^{(1)}$ is defined exatly as in equation (7). It can be seen that Projected soil temperature is a better tracer of surface soil moisture than ground-based soil temperature. In particular, the projection makes the low values of soil temperature observed in (a) increase so that the correlation soil temperature/soil moisture is generally improved in (b).

However, the errorbars of Projected soil temperature $\overline{T_s^m}^{(1)}$ computed for each METFLUX site and each PBMR mission are relatively high. This effect is assumed to be attributed to relatively high variations in solar radiation within the input dataset. To test this assumption, another projection technique named projection 2 is proposed. Projected soil temperature $\overline{T_s^m}^{(2)}$ is defined by replacing in (7) the local surface conditions Y^m by $Y^{(2)}$. The new surface conditions $Y^{(2)}$ are written as:

$$Y^{(2)} = (< S >, T_a, Rh_a, u_a, sand, A, B, h_c, LAI) \tag{14}$$

with $< S >$ the aggregated solar radiation (average of the local solar radiation S^m). In Figure 4 are plotted in (b) Projected soil temperature $\overline{T_s^m}^{(1)}$ versus surface soil moisture and in (c) Projected soil temperature $\overline{T_s^m}^{(2)}$ versus surface soil moisture. It can be seen that the standard deviation of Projected soil temperature $\overline{T_s^m}^{(2)}$ is much lower than the standard deviation of Projected soil temperature $\overline{T_s^m}^{(1)}$. This result is due to the errors introduced by

LS model when simulating soil temperature in a wide range of solar radiation. It is suggested that the soil temperature simulated by LS model is not exactly consistent with the soil temperature measured at -2.5 and -5.0 cm: LS model simulates the soil skin temperature. The simulated soil temperature is therefore more sensitive to solar radiation than the ground-based soil temperature measured at several centimeters below the soil surface.

It is shown that Projected soil temperature $\overline{T_s^m}^{(2)}$ is a better tracer of the spatial variability of surface soil moisture than ground-based soil temperature and is more robust to uncertainity in surface conditions (especially solar radiation) than the Projected soil temperature obtained with projection technique 1. Projection technique 2 is therefore chosen for the application of the downscaling method in the next section.

5.3 Results

The downscaling method is applied to the six microwave pixels generated from the Monsoon '90 data. For each day of PBMR mission, the downscaling method is run 240 times on the noisy input dataset and the performance of the approach is tested by comparing the downscaled soil moisture to ground-based measurements at the eight METFLUX sites.

Results are illustrated in Figure 5 where the ground-based soil temperature T_s^m, the Projected soil temperature $\overline{T_s^m}$ and the downscaled soil moisture W are successively plotted versus ground-based soil moisture W^m for each METFLUX site and each PBMR mission. A good agreement is generally observed between the downscaled soil moisture and ground-based measurements. On

JD 214 however, the spatial variability of surface soil moisture is not as well represented as for the other days.

In Table 3 are presented for each PBMR mission the mean and the standard deviation of the error SD (%) between the downscaled and ground-based soil moisture, the aggregated solar radiation $< S >$ (W/m^2), the inverted microwave scale soil moisture W_{SMOS}^{inv} (%) and the inverted contrast parameter f_1^{inv} (%/K). It can be seen that the aggregated solar radiation $< S >$ is relatively low (651 W/m^2) on JD 214. In fact, the value of solar radiation at microwave resolution is likely to affect the robustness of the downscaling method. When solar radiation is globally high within the microwave pixel, the contrast in soil temperature is also relatively high so that the spatial variability of soil temperature can be used to describe the spatial variability of surface soil moisture. However, when solar radiation is globally low within the microwave pixel, the ratio "variability of soil temperature due to some heterogeneity in surface soil moisture"/"measurement noise on soil temperature" is also low, which results in high deviations on the downscaled soil moisture.

6 Conclusion

A downscaling method of the surface soil moisture extracted from a SMOS type pixel is applied to the Monsoon '90 data. The aircraft-based L-band PBMR data obtained on Julian days 212, 214, 216, 217, 220 and 221 are aggregated to generate a time-series of heterogeneous microwave pixels. Each microwave pixel is composed of eight sub-pixels corresponding to the PBMR pixels located at the eight METFLUX stations operating over the study area.

The microwave soil moisture is downscaled in two successive steps. In a first step, the local information provided by the eight METFLUX stations (ground-based soil temperature, atmospheric conditions, soil and vegetation characteristics) are used to describe the spatial variability of surface soil moisture within the microwave pixel. A soil moisture distribution is then expressed as function of two parameters: the microwave scale soil moisture W_{SMOS} and a first-order parameter f_1 called the contrast parameter of the distribution. In a second step, the distribution of surface soil moisture obtained in step 1 is calibrated at the scale of the microwave pixel by inverting both parameters W_{SMOS} and f_1 from bi-angular microwave observation.

The performance of the approach is tested by comparing the output downscaled soil moisture to ground-based measurements at each METFLUX site and for each day of PBMR mission. The results show a good agreement between the downscaled and measured surface soil moisture as long as the intensity of solar radiation is sufficiently high (above 700 Wm^{-2}) to use ground-soil soil temperature as a tracer of the spatial variability of surface soil moisture. The application to the Monsoon '90 data clearly shows that the downscaling method should be used for clear sky conditions, when solar radiation is globally high within the microwave pixel. Note that this limitation should not be an issue in the operational case since the thermal infrared data from which the soil temperature is derived are available only for clear sky conditions.

In this application, an empirical radiative transfer model first parameterized with aircraft-based data was successfully used by the disaggregation method. The point is such a parameterization may be difficult to develop under different surface conditions, over large areas and over time periods longer than the 10-days period of PBMR data. To overcome these limitations, physically-based

radiative transfer models should be used in the future, with a particular focus on the modeling of angular effects.

Besides, to fully assess the robustness of the method on an operational basis, the algorithm needs to be tested with radiometric soil temperature. This is an important issue because the radiometric soil temperature may be not as sensitive to the 0–5 cm soil moisture as the ground-based -2.5 cm soil temperature used in the paper.

In the future, the sequential assimilation of the microwave data disaggregated by such a downscaling method will provide some information about the spatial and temporal variation in the near-surface and root-zone soil moisture. This will be a critical issue for achieving efficient and sustainable water use.

Acknowledgement

The authors would like to thank William Kustas, Susan Moran and Tom Schmugge for making the Monsoon '90 data available. The necessary financial support to conduct the Monsoon '90 field experiment is also acknowledged: funds from NASA Interdisciplinary Research Program in Earth Sciences (NASA Reference No. IDP-88-086) and funds from the USDA-ARS Beltsville Area Office. This work was supported by a grant from CNES and CNRS and the CNES program TOSCA.

References

Bindlish, R., Barros, A. P., february 2002. Subpixel variability of remotely sensed soil moisture: An inter-comparison study of SAR and ESTAR. IEEE Trans. Geosci. Remote Sens. 40, 326–337.

Brunfeldt, D. R., Ulaby, F. T., 1984. Measured microwave emission and scattering in vegetation canopies. IEEE Trans. Geosci. Remote Sens. 22, 520–524.

Chauhan, N. S., Miller, S., Ardanuy, P., 2003. Spaceborne soil moisture estimation at high resolution: a microwave-optical/IR synergistic approach. Int. J. Remote Sens. 24 (22), 4599–4622.

Daughtry, C. S. T., Weltz, M. A., Perry, E. M., Dulaney, W. P., 1991. Direct and indirect estimates of leaf area index. In: Tenth Conference on Biometeorology and Aerobiology; Special Session on Hydrometeorology, Am. Meteorol. Soc. Salt Lake City, Utah.

Engman, T., 1991. Application of remote sensing of soil moisture for water resources and agriculture. Remote Sens. Environ. 35, 213–226.

Entekhabi, D., Asrar, G. R., Betts, A. K., Beven, K. J., Bras, R. L., Duffy, C. J., Dunne, T., Koster, R. D., Lettenmaier, D. P., McLaughlin, D. B., Shuttleworth, W. J., van Genuchten, M. T., Wei, M.-Y., Wood, E. F., 1999. An agenda for land surface hydrology research and a call for the Second International Hydrological Decade. Bull. Am. Meteorol. Soc. 80 (10), 2043–2058.

Jackson, T. J., Vine, D. M. L., Hsu, A. Y., Oldak, A., Starks, P. J., Swift, C. T., Isham, J. D., Haken, M., september 1999. Soil moisture mapping at regional scales using microwave radiometry: The Southern Great Plains Hydrology Experiment 37 (5), 2136–2151.

Kerr, Y. H., Waldteufel, P., Wigneron, J.-P., Martinuzzi, J.-M., Font, J., Berger, M., august 2001. Soil moisture retrieval from space: the soil moisture and ocean salinity (SMOS) mission. IEEE Trans. Geosci. Remote Sens. 39, 1729–1735.

Kim, G., Barros, A. P., 2002. Downscaling of remotely sensed soil moisture with a modified fractal interpolation method using contraction mapping and ancillary data. Remote Sens. Environ. 83, 400–413.

Kustas, W. P., Goodrich, D. C., 1994. Monsoon '90 multidisciplinary experiment. Water Resources Res. 30 (5), 1211–1225.

Kustas, W. P., Goorich, D. C., Moran, M. S., Amer, S. A., Bach, L. B., Blanford, J. H., Chehbouni, A., Claassen, H., Clements, W. E., Doraiswamy, P. C., Dubois, P., Clarke, T. R., Daughtry, C. S. T., Gellman, D. I., Grant, T. A., Hipps, L. E., Huete, A. R., Humes, K. S., Jackson, T. J., Keefer, T. O., Nichols, W. D., Parry, R., Perry, E. M., Pinker, R. T., Pinter, P. J., Qi, J., Riggs, A. C., Schmugge, T. J., Shutko, A. M., Stannard, D. I., Swiatek, E., van Leeuwen, J. D., van Zyl, J., vidal, A., Washburne, J., Weltz, M. A., 1991. An interdisciplinary field study of the energy and water fluxes in the atmosphere-biosphere system over semiarid rangelands: Description of some preliminary results. Bull. Am. Meteorol. Soc. 72, 1683–1705.

Kustas, W. P., Norman, J. M., 1999. Evaluation of soil and vegetation heat flux predictions using a simple two-source model with radiometric temperatures for partial canopy cover. Agr. For. Meteorol. 94, 13–29.

Kustas, W. P., Zhan, X., Schmugge, T. J., 1998. Combining optical and microwave remote sensing for mapping energy fluxes in a semiarid watershed. Remote Sens. Environ. 64, 116–131.

Merlin, O., Chehbouni, G., Kerr, Y., Njoku, E. G., Entekhabi, D., 2005. A combined modeling and multi-spectral/multi-resolution remote sensing ap-

proach for disaggregation of surface soil moisture: Application to SMOS configuration. IEEE Trans. Geosci. Remote Sens. 43 (9), 2036–2050.

Mo, T., Choudhury, B. J., Schmugge, T. J., Wang, J. R., Jackson, T. J., 1982. A model for microwave emission from vegetation-covered fields. J. Geophys. Res. 87 (13), 11229–11237.

Noilhan, J., Mahfouf, J.-F., 1996. The ISBA land surface parameterisation scheme. Glob. Planet. Change 13, 145–159.

Norman, J. M., Kustas, W. P., Humes, K. S., 1995. Source approach for estimating soil and vegetation energy fluxes in observations of directional radiometric surface temperature. Agr. For. Meteorol. 77, 263–293.

Pellenq, J., Kalma, J., Boulet, G., Saulnier, G.-M., Wooldridge, S., Kerr, Y., Chehbouni, A., may 2003. A disaggregation scheme for soil moisture based on topography and soil depth. J. Hydrol. 276, 112–127.

Schmugge, T., Jackson, T. J., Kustas, W. P., Roberts, R., Parry, R., Goodrich, D. C., Amer, S. A., Weltz, M. A., 1994. Push broom microwave radiometer observations of surface soil moisture in Monsoon '90. Water Resour. Res. 30 (5), 1321–1327.

Sellers, P. J., Heiser, M. D., Hall, F. G., 1992. Relations between surface conductance and spectral vegetation indices at intermediate (100 m^2 to 15 km^2) length scales. J. Geophys. Res. 97 (D17), 19033–19059.

Ulaby, F. T., Moore, R. K., Fung, A. K., 1986. Microwave Remote Sensing - Active and Passive. Vol. 3. Artech House, Norwood, MA.

Weltz, M. A., Ritchie, J. C., Fox, H. D., 1994. Comparison of laser and field measurements of vegetation height and canopy cover. Water Resour. Res. 30 (5), 1311–1319.

Wigneron, J.-P., Waldteufel, P., Chanzy, A., Calvet, J.-C., Kerr, Y., 2000. Two-dimensional microwave interferometer retrieval capabilities over land

surfaces (SMOS mission). Remote Sens. Environ. 73, 270–282.

Table 1

Date, time and cloud cover conditions of the 6 PBMR flights during the Monsoon '90 experiment.

Julian day	Time (MST)	Cloud cover
212	0930-1110	Mostly clear skies
214	0915-1040	Overcast skies
216	0825-0940	High cirrus clouds
217	1000-1100	Partly cloudy - Cirrus
220	0900-0915	Clear skies
221	1010-1115	Clear skies

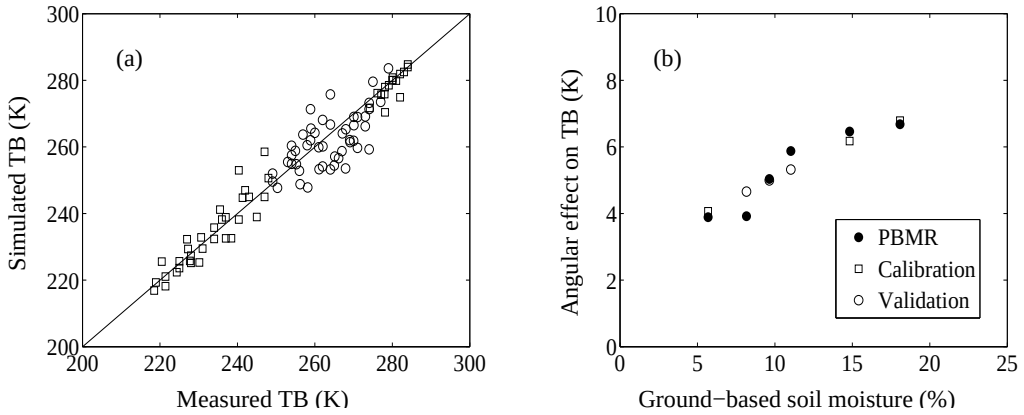

Fig. 1. Calibration results in terms of the simulated angular (nadir and oblique) brightness temperature and the simulated angular effect evaluated as the daily nadir-oblique brightness temperature difference.

Table 2

Calibration parameters estimated over the eight sub-pixels composing the generated microwave pixel.

Sub-pixel	$a^{\perp}$	$b^{\perp}$	$a^{\angle}$	$b^{\angle}$	A	B
1	−8.50	328.45	−8.88	326.78	7.0	8.5
2	−3.55	302.39	−3.71	299.31	6.0	3.5
3	−4.19	295.56	−4.42	292.51	6.5	6.5
4	−2.05	290.68	−2.18	287.15	7.0	5.5
5	−5.49	341.13	−5.90	341.45	8.0	9.5
6	−6.23	321.60	−6.58	319.80	7.0	9.0
7	−3.92	292.21	−4.12	288.66	6.0	5.0
8	−3.10	290.54	−3.26	287.10	6.5	3.0

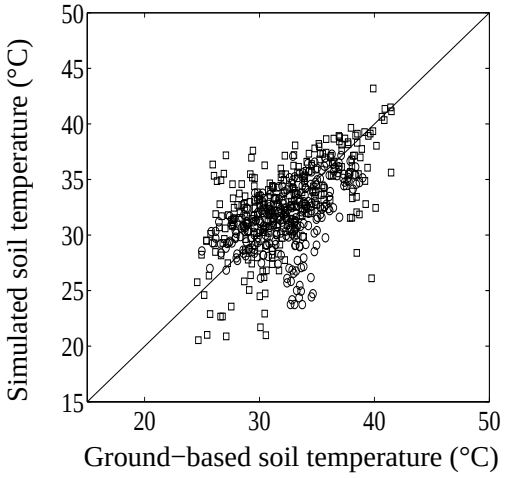

Fig. 2. Soil surface temperature simulated by LS model versus ground-based measurements (□: JD 212-216; ○: JD 217-221).

Table 3

Mean and standard deviation of: the error SD between the downscaled and measured soil moisture, the aggregated solar radiation $< S >$, the inverted microwave-scale soil moisture W_{SMOS}^{inv} and the inverted contrast parameter f_1^{inv}. The statistical results were computed with 240 independent datasets for each of the six microwave pixels.

	Error	Aggregated solar radiation	Inverted microwave-scale soil moisture	Inverted contrast parameter
	SD (%)	$< S >$ (Wm^{-2})	W_{SMOS}^{inv} (%)	f_1^{inv} (%/K)
Julian day	Mean (SD)	Mean (SD)	Mean (SD)	Mean (SD)
212	1.1 (0.34)	872 (67)	5.7 (0.04)	−0.89 (0.20)
214	6.9 (2.4)	647 (223)	16.5 (0.05)	−4.3 (1.4)
216	4.5 (0.8)	882 (86)	14.6 (0.05)	−3.0 (0.73)
217	3.8 (0.86)	761 (167)	9.3 (0.05)	−3.5 (1.0)
220	3.5 (0.70)	852 (56)	10.5 (0.03)	−1.8 (0.58)
221	1.5 (0.41)	887 (36)	7.5 (0.02)	−1.8 (0.51)

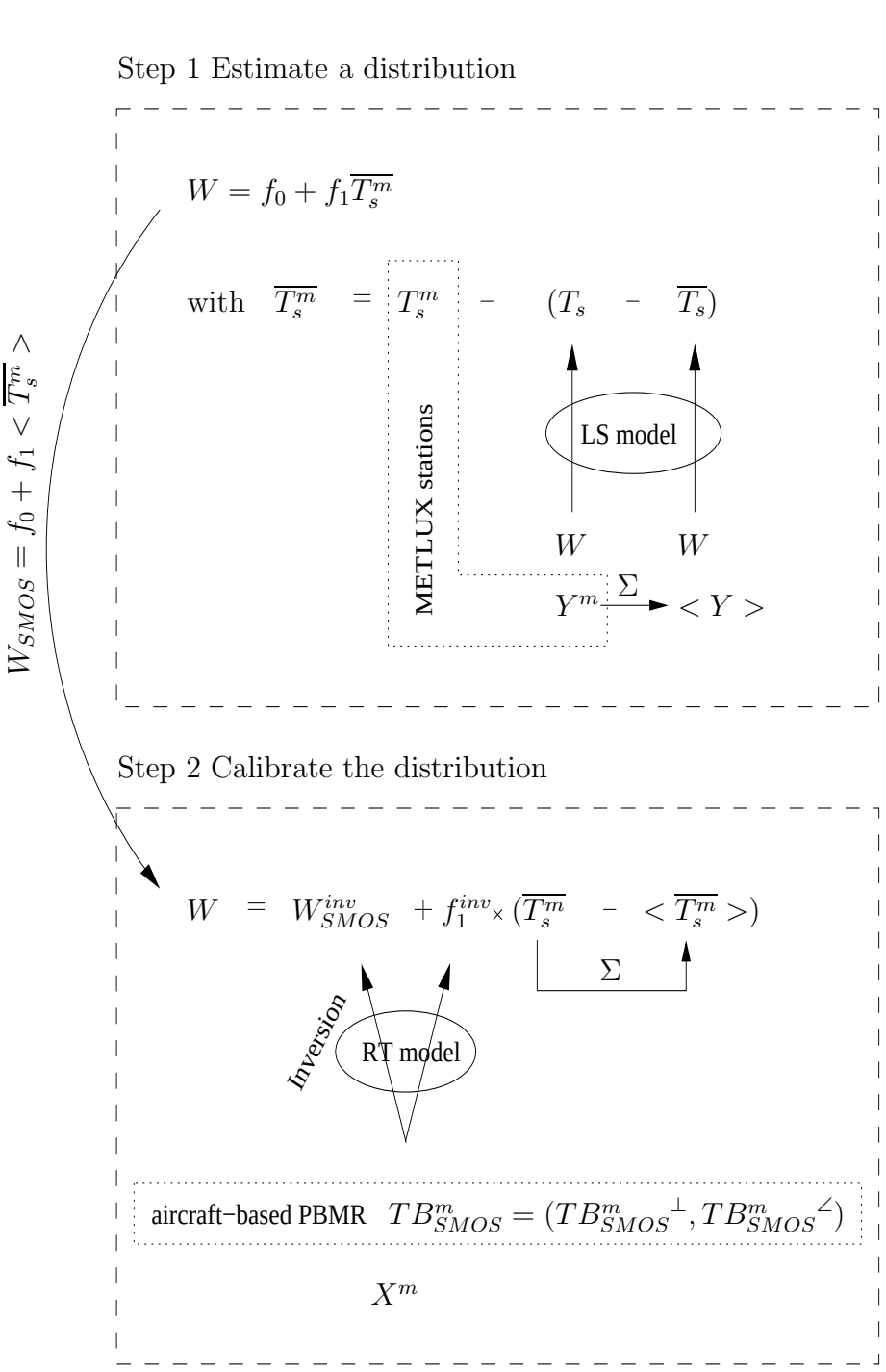

Fig. 3. The two successive steps of the method are presented. In step 1, a spatial distribution of surface soil moisture is estimated from ground-based soil temperature T_s^m and from LS model predictions giving the contribution of the ground-based soil temperature due to surface conditions' heteorogeneity $(T_s - \overline{T_s})$. The downscaled soil moisture is then a function of two parameters defined at microwave resolution f_0 and f_1. In step 2, the local relationship derived in step 1 is re-written at microwave scale to make the coarse resolution soil moisture W_{SMOS} appear in the expression. Both parameters W_{SMOS} and f_1 are then inverted from bi-angular microwave observation to calibrate the distribution.

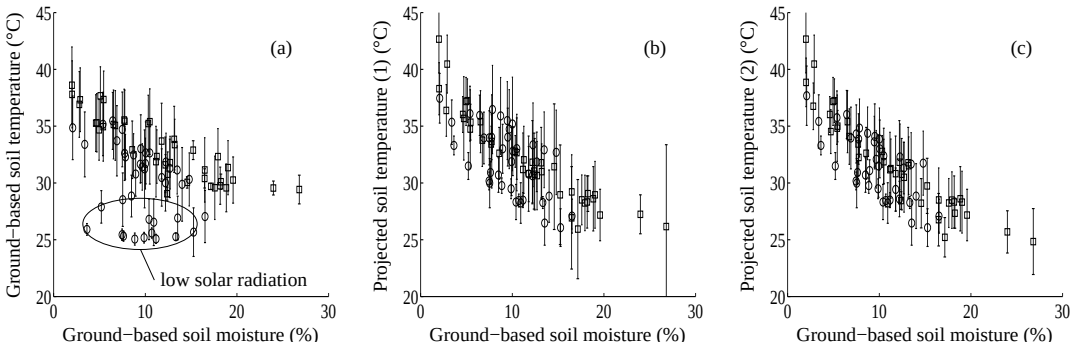

Fig. 4. Comparison of the correlation between soil temperature and ground-based soil moisture for three different soil temperatures: (a) ground-based soil temperature T_s^m, (b) the soil temperature $\overline{T_s^m}^{(1)}$ obtained with projection technique 1 and (c) the soil temperature $\overline{T_s^m}^{(2)}$ obtained with projection technique 2. The mean and the standard deviation of the 12 soil temperature values associated with a given METFLUX site on a given day between JD 212 and JD 221 are represented (□: JD 212-216; ∘: JD 217-221).

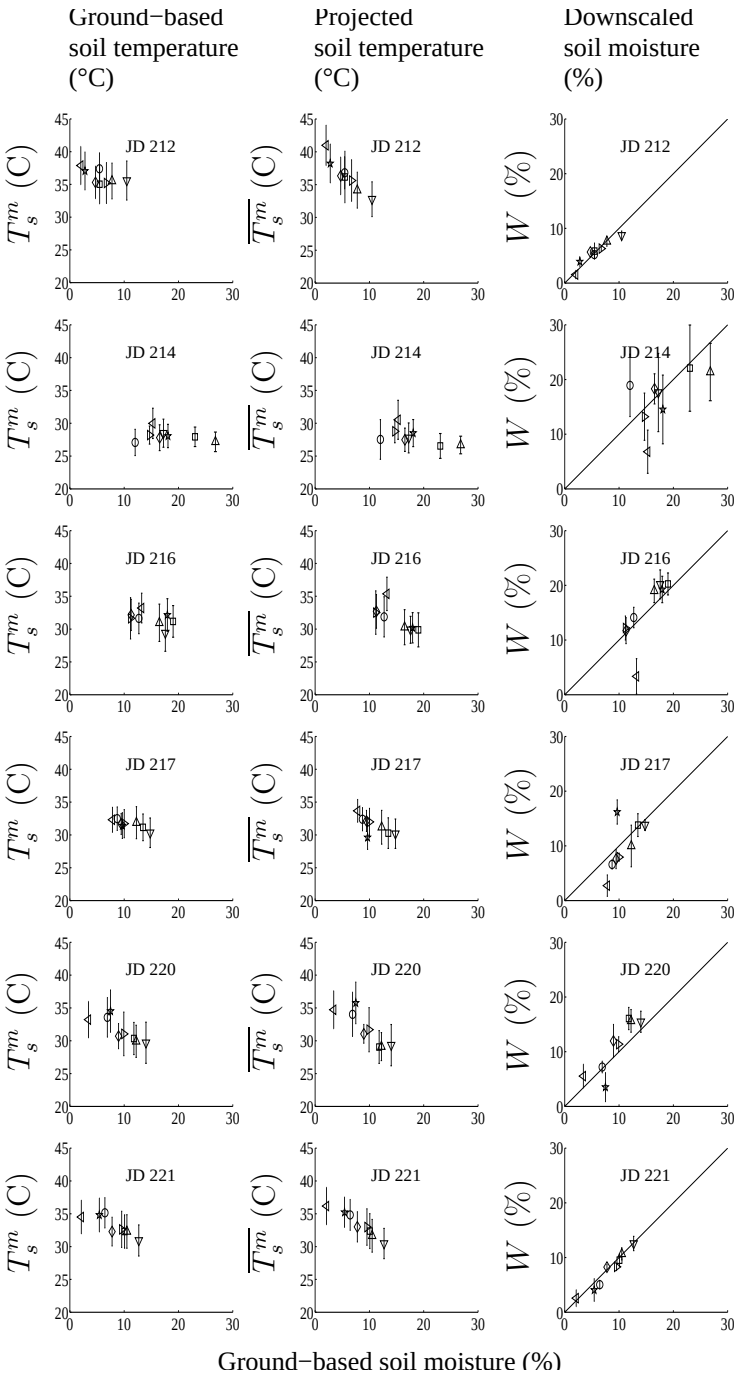

Fig. 5. Results of the application of the downscaling method to the six microwave pixels. For each PBMR mission, ground-based soil temperature, Projected soil temperature and the downscaled soil moisture are successively plotted versus ground-based soil moisture. Mean and standard deviation are provided for each METFLUX site to show the sensitivity of the method to uncertainity in input data ($\circ$: site 1; $\square$: site 2 ; $\diamond$: site 3; $\triangle$: site4; $\bigtriangledown$: site5; $\triangleright$: site 6; $\triangleleft$: site 7; $\star$: site 8).